Equilibrium Flexibility of a Rigid Linear Conjugated Polymer

Patricia M. Cotts*,†

IBM Research Division, Almaden Research Center, San Jose, California 95120

Timothy M. Swager and Qin Zhou

Department of Chemistry and Laboratory for Research on the Structure of Matter, University of Pennsylvania, Philadelphia, Pennsylvania 19104

Received February 15, 1996; Revised Manuscript Received July 29, 1996[⊗]

ABSTRACT: The unusual electronic and optical properties of many electroluminescent and conducting polymers arise from extended conjugation along the polymer backbone, which can also lead to insolubility, aggregation, and gelation. Synthetic efforts to produce an optimal structure require a balance between the persistence length and the effective conjugation length for the successful implementation of these materials in photonic and electronic devices. In this study, we have investigated the solution properties of a group of poly(phenyleneethynylenes) using a variety of light scattering techniques, including polarized and depolarized intensity measurements, dynamic light scattering, and size exclusion chromatography with a multiangle light scattering detector (SEC/LS). Interpretation of light scattering in the presence of absorption, fluorescence, and optical anisotropy is discussed. The molecular weights determined by light scattering encompassed the range from 10×10^5 to 5×10^6, with the root-mean-square radius of gyration as high as 250 nm. The results may be interpreted with a wormlike chain model to yield a persistence length of about 15 nm, so that these high-*M* polymers are coil-like in solution, rather than "rigid rods". This persistence length is still expected to be several times larger than the effective conjugation length.

Introduction

Polymers which are characterized by a high degree of conjugation along the polymer backbone display a variety of electronic and optical properties which provide opportunities for application in electroluminescent displays,[1] fluorescent chemosensors,[2] nonlinear optics, photoconductors, and a variety of emerging electronic and photonic devices.[3−5] The full implementation of these materials requires an optimization of their structural, electronic, and optical properties. While characterization of the unusual optical and electronic behavior has received much attention,[6,7] less effort has been devoted to the understanding of the equilibrium structure in solution.[8−10] Extensive backbone conjugation, which produces intriguing electronic properties, also results in more complex solution behavior. In many cases, the conjugated polymers are not soluble in any common organic solvent, and even when some solubility is achieved, strong intermolecular interactions among the polymers can lead to aggregation and gelation.[11] In addition to complicating the solution characterization of these materials, these interactions also affect the processing and ultimate film behavior.

In this study, we have investigated the single-molecule structure of a soluble conducting poly(phenyleneethynylene) using a variety of light scattering techniques. The highly conjugated phenyleneethynylene backbone is substituted with both ether and amide alkyl side chains, which results in this polymer being soluble in common organic solvents such as chloroform and tetrahydrofuran (THF).[12,13] The polymer has been developed primarily as a fluorescent chemosensor, and the exceptionally high molecular weights obtained resulted in enhanced sensitivity.[13] Hereafter we refer to this polymer simply as QZ.

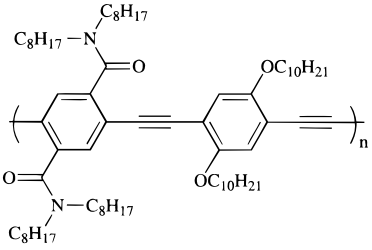

QZ

Preliminary molecular weight characterization of synthetic polymers is usually accomplished using size exclusion chromatography (SEC). The typical SEC measurement is only a relative measure of *M*, whereas light scattering can provide an absolute molecular weight. Both the intensity of the light scattered and the viscosity of a solution depend on the molecular weight of the polymer as well as the concentration in the solution. In the case of the light scattering detector, the "true" molecular weight of each fraction across the distribution is obtained when both the concentration and differential refractive index increment (d*n*/d*c*) are known. When the detector is equipped to measure several scattering angles, both the molecular weight and the root-mean-square radius of gyration (R_g) may be determined independently across the distribution. This provides a powerful tool for determining the equilibrium structure of a polymer in solution with only a few milligrams of sample.

Highly conjugated polymers such as QZ are often optically anisotropic and exhibit significant depolarized scattering, even at fairly high *M*. In the presence of significant depolarized scattering, the usual expressions to obtain *M* and R_g from light scattering are modified to include the anisotropy factor, δ. Determination of an average δ for the lowest *M* sample of QZ (δ is inversely dependent on *M* for coil-like molecules) was accomplished using a low-angle light scattering instrument as described below. The QZ solutions in THF or chloroform are colored (yellow) and fluoresce strongly

† Present address: DuPont CR&D, Experimental Station, Wilmington, DE 19880.

[⊗] Abstract published in *Advance ACS Abstracts,* October 1, 1996.

S0024-9297(96)00258-6 CCC: $12.00

in the blue under ambient light. Experimental considerations to eliminate contributions of absorption and fluorescence to the light scattering are discussed in detail below.

Experimental Methods

Materials. The synthesis of the QZ polymers was previously described.[13] The solvents, THF and $CHCl_3$, were reagent or HPLC grade (THF was stabilized with BHT) and were used as received. Solutions were filtered through a 0.5 μm Fluoropore filter prior to SEC/LS or off-line LS measurements.

Low-Angle Light Scattering. The intensity of light scattered from dilute solutions of the lowest M sample (QZ1) in THF was measured using a KMX-6 low-angle light scattering photometer (Thermo-Separation Products). Solutions were filtered through a 0.5 μm Fluoropore filter (Millipore Corp.) directly into the KMX-6 cell. For this measurement, an analyzing polarizer was placed in front of the photomultiplier, so that the scattered intensity could be measured with the analyzer oriented parallel (V_v) or perpendicular (H_v) to the vertically polarized incident beam. The orientation and polarization of the analyzer were confirmed by measurements on pure solvents (toluene and chloroform) for which the anisotropy factors are known.[14]

In the limit of infinite dilution, and zero scattering angle, the anisotropy factor, δ, and the weight-average molecular weight may then be evaluated using[15]

$$\rho_v \equiv \frac{R_{H_v}}{R_{H_v}} = \frac{3\delta}{1+4\delta} \tag{1}$$

where R_{H_v} and R_{V_v} are the excess (minus the solvent) depolarized and polarized Rayleigh factors, respectively, extrapolated to infinite dilution. M_w may be evaluated using

$$\frac{Kc}{R_{V_v}} = \frac{1}{M(1+4\delta)} \tag{2}$$

where

$$K = \frac{4\pi^2 n^2 (\mathrm{d}n/\mathrm{d}c)^2}{\lambda^4 N_A} \tag{3}$$

with dn/dc the refractive index increment, n the refractive index (1.404 for THF), and λ the vacuum wavelength of light (632.8 nm).

The QZ solutions are highly colored and exhibit fluorescence in the visible range. Significant absorption effects can be observed under these conditions even when the wavelength of the incident light is far from the maximum in the electronic absorption spectrum, since the concentrations used for light scattering are typically much larger than for spectroscopic measurements.[16] For the QZ solutions, the maximum occurs at 422 nm, and the incident wavelength for light scattering measurements is 632.8 nm. The transmitted intensity was used as a measure of the incident intensity in the evaluation of R_θ to compensate for any absorption at 632.8 nm. Contributions of fluorescence to the measured scattering intensity were minimized by use of a 10 nm bandwidth interference filter centered at 632.8 nm placed before the detector.

Size Exclusion Chromatography with a Multiangle Light Scattering Detector. SEC measurements were accomplished using a modular instrument consisting of a Waters 590 pump, a Waters WISP automatic sample injector, and a Dawn Model DSP multiangle light scattering detector. A set of two size exclusion columns (PLGel, mixed A, 20 μm particle size, Polymer Laboratories) appropriate for very high molecular weights was used and housed in an oven thermostated at 40 °C. The mobile phase was either HPLC grade THF or $CHCl_3$ which were filtered and degassed by vacuum filtration through a 0.5 μm Fluoropore filter prior to use. Solutions were prepared at about 1 mg/mL concentration. Unlike standard SEC, SEC/LS measurements require that the mass eluting at each point on the chromatogram be known accurately. This may be accomplished either by (1) knowing the mass injected and assuming all the polymer elutes from the column (*mass* method) and/or (2) using the calibrated differential refractive index detector with a known dn/dc to measure the mass concentration of the polymer as it elutes (dn/dc method). For this series the QZ polymers, most of the samples were not completely soluble in THF or $CHCl_3$. The incompletely dissolved polymer samples were filtered through a 0.5 μm Fluoropore filter, and the concentration of the filtered solution was determined by UV−visible spectroscopy. The polymer solutions display a characteristic electronic absorption spectrum with a maximum at 422 nm, resulting in the yellow color of the solutions. The extinction coefficient at 422 nm, as well as the dn/dc, was determined using a series of concentrations of some of the lower molecular weight polymers, which were completely soluble. The experimental values for dn/dc (mL/g) were were 0.163 (THF) and 0.136 ($CHCl_3$), and the extinction coefficient (ϵ (M^{-1}) at 422 was 4.2×10^4. For all samples measured, the concentrations calculated by the mass method and the dn/dc method agreed within 1−2%. The weight-average molecular weights (M_w) and the polydispersity obtained for the *soluble, filtered solutions* are listed in Table 1.

Table 1. Nominal Molecular Weights of QZ Polymers[a]

	M_w	M_w/M_n
QZ1	270000	2.5
QZ2	530000	2.4
QZ3	500000	1.8
QZ4	300000	1.4
QZ5	800000	2
QZ6	2000000	2

[a] Values of M_w and M_w/M_n reflect the average of the *soluble, filtered solutions* measured in THF and $CHCl_3$.

Dynamic Light Scattering. Dynamic light scattering was used to determine the average translational diffusion coefficient, D, at infinite dilution for the lowest molecular weight sample, QZ1. A Brookhaven system was used, consisting of a BI 200 SM automatic goniometer and a BI9000 AT correlator. The incident light was provided by a Spectra-Physics Model 27 He−Ne laser. The same solutions which were used for the low-angle intensity measurements were filtered into 16 mm diameter culture tubes which had been cleaned by inverting them over refluxing 2-propanol for several hours. For $\theta < 60°$, the first cumulant, Γ, displayed a linear dependence on q^2, where q is the scattering vector $q = (4\pi n/\lambda)\sin(\theta/2)$. Subsequent concentrations were measured at 45° scattering angle. Deviations from a linear dependence at higher q ($qR_g > 1$) are expected due to contributions from internal motions of the polymer coil, rotational diffusion, and polydispersity.

Results

Low-Angle Intensity Light Scattering. The V_v and H_v components of the reciprocal scattering intensity at 4° scattering angle are shown in Figure 1 as a function of concentration of QZ1 in THF. Both components display a moderate positive dependence on concentration, indicating a positive thermodynamic polymer−solvent interaction, at least at this lower M. The limited solubility observed for some of the samples might be an indication of some equilibrium of polymer-rich and polymer-poor phases as a function of M. The limited solubility might also be a manifestation of a kinetic insolubility. Strong kinetic effects are common in highly extended conjugated polymers, for which even van der Waals interactions between polymer segments are strongly propagated along the extended polymer chain.[8−9,11,17] The depolarization ratio ρ_v, defined in eq 1, is 0.05 and was independent of concentration (within experimental uncertainty) for the very dilute range of concentrations measured. This small depolarization ratio results in a maximum correction of about 7% in the M_w determined by light scattering. The weight-average molecular weight, M_w, corrected for optical anisotropy as described above is 270 000.

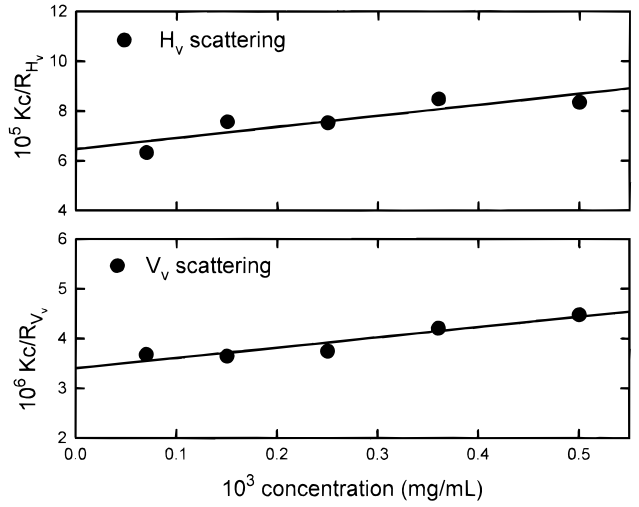

Figure 1. Polarized (V_v) and depolarized (H_v) intensity scattering from solutions of QZ1 as a function of concentration.

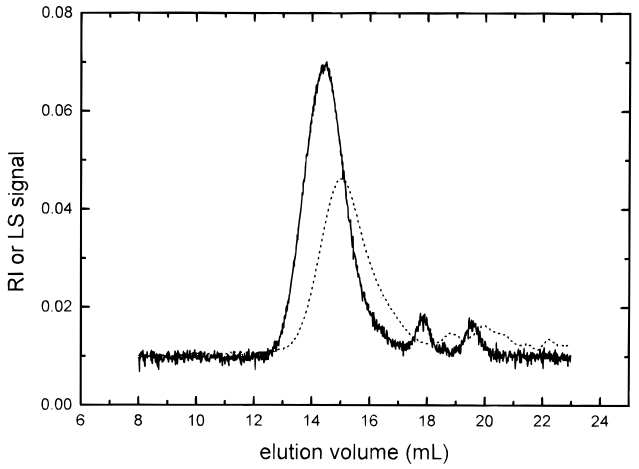

Figure 2. Refractive index (RI) and 90° light scattering (LS) chromatograms for QZ2.

SEC/LS. SEC/LS measurements were done on the soluble portions of the six whole polymers in both THF and $CHCl_3$. Molecular weight distributions obtained for the higher M samples were narrower (typically, $M_w/M_n = 1.5$) than those obtained for the completely soluble lower M samples ($M_w/M_n = 2.3$), indicating that some fractionation occurred with the incomplete solubility. A representative dual chromatogram is shown in Figure 2 for QZ2 with both the refractive index and light scattering intensity at 90° shown as a function of elution volume. As is expected for broad distribution polymers, the light scattering intensity is skewed toward the high-M, earlier elution portion of the distribution, since the scattering intensity is proportional to the product of the concentration c and the molecular weight M. The Dawn DSP is a multiangle light scattering instrument, so that light scattering intensity chromatograms are obtained at 18 different scattering angles, covering the range from $14° < \theta < 152°$ for THF. A 3-D plot showing the changes in the light scattering intensity chromatograms as a function of scattering angle for QZ6 in $CHCl_3$ is shown in Figure 3. For this highest M sample, the decrease in scattering intensity at higher scattering angles due to destructive intramolecular interference is dramatic. Evaluation of the molecular weight and root-mean-square radius of gyration, R_g, at each elution volume requires extrapolation of the reciprocal intensities as a function of scattering angle to zero scattering angle as shown in Figure 4 for QZ2. The very high dilutions used in SEC/LS usually are sufficient so that

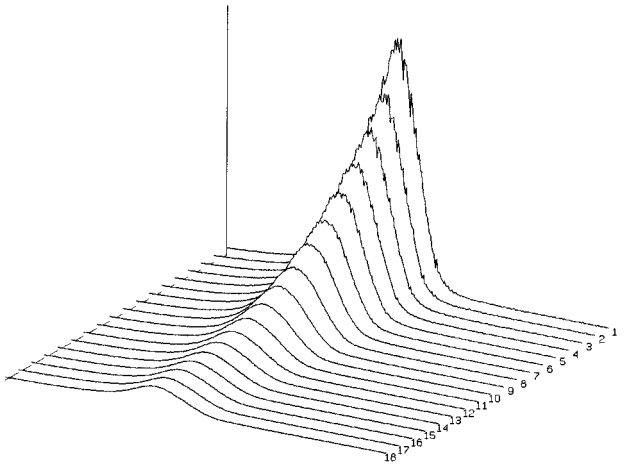

Figure 3. 3-D plot of the chromatograms for the RI and from all 18 LS detectors for QZ6.

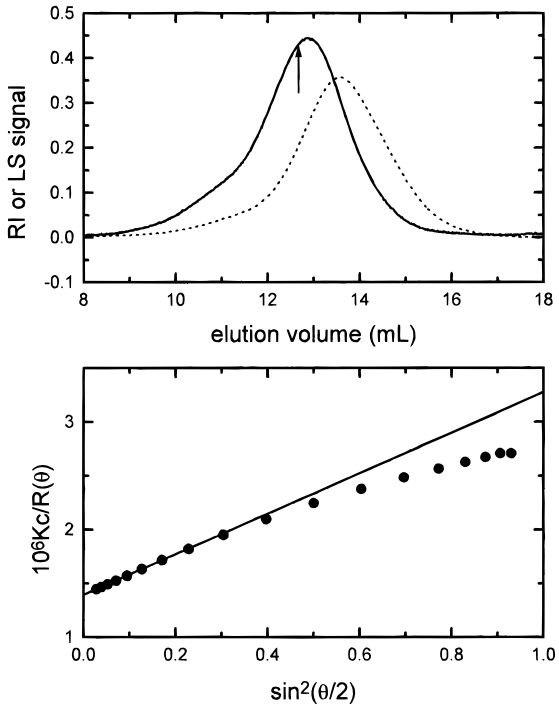

Figure 4. Debye plot of Kc/R_θ as a function of $\sin^2(\theta/2)$ for a single slice of the QZ2 distribution as shown.

no extrapolation to infinite dilution is required. The molecular weight M and R_g are then evaluated using the usual expression:[18]

$$\frac{Kc}{R_\theta} = \frac{1}{M} + \frac{q^2 R_g^2}{3} + \dots \qquad (4)$$

where q and K are as defined earlier. The molecular weight distribution at each elution volume is sufficiently narrow that the various averages, M_n, M_w, etc., are the same within the experimental uncertainty. The averages M_w and M_n (as well as $R_{g,z}$, $R_{g,w}$, etc.) for the entire distribution may then be calculated through the usual summations. Since many of the samples were not completely soluble, we do not report the polydispersity information here. QZ1, which was completely soluble, had a polydispersity index, M_w/M_n, of 2.5. The M_w calculated for this sample from the SEC/LS data was within 5% of that obtained from the low-angle light scattering on the unfractionated polymer when corrected for optical anisotropy as described above.

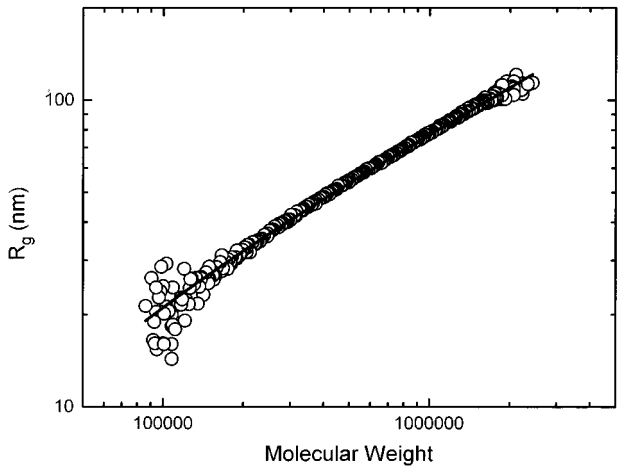

Figure 5. log−log plot of R_g vs M for slices across the distribution of QZ4, along with a fitted curve for a wormlike chain.

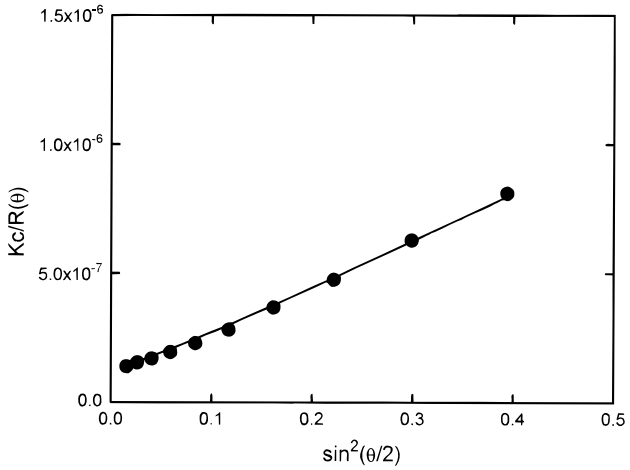

Figure 6. Kc/R_θ as a function of $\sin^2(\theta/2)$ for a very high M slice of QZ6, along with the fit to the Debye function (eq 5 in text).

In classical polymer light scattering, the polydispersity of the sample can be problematic, since the averages measured for the molecular weight (M_w) and the root-mean-square radius of gyration ($R_{g,z}$) differ. However, with SEC/LS, a broad molecular weight distribution can be beneficial, since it results in determination of R_g and M for narrow distribution "fractions" over a wide molecular weight range. An example is QZ4 in THF (Figure 5), where the molecular weight range extends for a decade using a single sample. Similar results were obtained for the other samples measured and also for measurements in $CHCl_3$.

Evaluation of R_g for the higher M samples and also for the higher M slices requires more detailed comment. Equation 4 is only valid in the Guinier region of Kc/R_θ vs q, i.e., for $qR_g < 1.5$, so that the complete set of 18 angles can be used only for $R_g < 50$ nm. As very high molecular weight and consequently high R_g is approached, the number of detectors which can be used with eq 4 becomes very limited. The use of a second-order polynomial fit can also introduce additional systematic errors. As a result, we have chosen to fit the data with the well-known Debye expression for random coils:[19]

$$\frac{Kc}{R_\theta} = \frac{1}{MP(\theta)} \tag{5a}$$

where

$$P(\theta) = \frac{2}{u^2}(e^{-u} - 1 + u) \tag{5b}$$

with $u = q^2R_g^2$. The Debye function has been shown to be valid for polymer coils even in good solvents for $u < 10$.[20,21] With this constraint, the first 10 detectors may be used even for the highest M "slice" of QZ6, the highest M sample measured, as shown in Figure 6. For this very high M of 9 million, the fit to the Debye function yields a R_g of 209 nm, a coil diameter of nearly 0.5 μm. The exceptionally high dilution attainable in SEC/LS minimizes the contribution of *inter*molecular interference in the observed scattering function. The data shown in Figure 6 are at a concentration of 0.0028 mg/mL, or 3 ppm.

Dynamic Light Scattering. Figure 7 shows the q^2 dependence of the first cumulant in the expansion of the normalized field autocorrelation function in terms of q, Γ:[22]

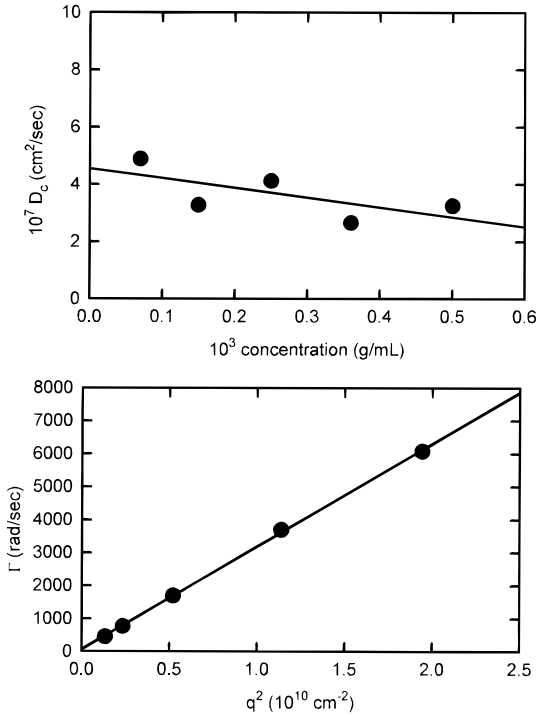

Figure 7. First cumulant, Γ, as a function of q^2 (lower plot) and D_c as a function of concentration (upper plot) for QZ1 in THF.

$$\ln g_1(t) = -\Gamma(t) + \frac{\mu_2 t^2}{2} \tag{6}$$

for the highest concentration of QZ1 measured, $c = 0.5$ mg/mL. The linear q^2 dependence observed for $qR_g < 0.5$ is confirmation that little or no contributions from internal modes or rotational diffusion are present. Subsequent measurements were done at $\theta = 45°$ scattering angle. D_c at each concentration c is then given by[23]

$$D_c = \frac{\Gamma}{q^2} \tag{7}$$

The second plot in Figure 7 shows D_c as a function of concentration yielding a limiting diffusion coefficient in infinite dilution, D_0, of 4.5 × 10^{-7} cm^2/s. Using the Stokes−Einstein relation

$$D_0 = \frac{kT}{6\pi\eta R_h} \quad (8)$$

with η the solvent viscosity, 0.55 cP for THF, yields an average hydrodynamic radius, R_h, of 11 nm. The concentration dependence of D_c is negative, although the intensity measurements shown in Figure 1 indicate a positive A_2. The concentration dependence of D_c reflects both A_2 and a frictional term, and negative slopes are expected for marginal solvents.

Discussion

Excluded Volume and Aggregation. The root-mean-square radius of gyration, R_g, values reported here have not been corrected for the effect of excluded volume interactions. While these interactions significantly increase the equilibrium dimensions of flexible polymer chains, the expected effect on semiflexible polymers is small since intrachain contacts are already greatly reduced. Assessments of the molecular weights above which excluded volume interactions become significant for a semiflexible chain vary widely,[24] but experimental results[25] indicate that excluded volume effects are not observed below about 50−100 Kuhn lengths, $M = 10^6$ for the QZ polymer.

The possibility of aggregation must also be considered for these polymers, especially since they were not all completely soluble. The consistency of the results in both $CHCl_3$ and THF as well as the static and dynamic light scattering is evidence that little contribution of aggregates is observed. The SEC/LS results showed no evidence for the presence of aggregates, and this technique is among the most sensitive for the detection of a small fraction of apparently high-M material. A final reassurance is provided by the fluorescence observed from these solutions—it is observed that aggregation leads to efficient quenching of fluorescence. The fluorescence could be eliminated from these solutions by addition of a nonsolvent, and the fluorescence disappeared prior to any visible turbidity or precipitation.

Distribution of Molecular Weight and Size. Figure 8 shows the distribution of R_g from SEC/LS data, and the *intensity-weighted* distribution of R_h from dynamic light scattering, for QZ1. While the R_g distribution is measured directly, the intensity-weighted distribution of R_h is obtained by an inverse Laplace transform of the measured autocorrelation function from dynamic light scattering. Since there are any number of distributions which will adequately reproduce the correlation function, the direct measurement of M and R_g using a chromatographic technique is far more reliable. The distribution of R_h shown in Figure 8 was obtained using a constrained regularization routine, REPES,[26] which uses the intensity correlation function, $g_2(t)$ rather than the field correlation, $g_1(t)$ used by several other commonly used routines such as CONTIN.[27] Results obtained using CONTIN were very similar to those obtained using REPES. The distribution from the inverse Laplace transform is an intensity-weighted distribution, which reflects the more intense scattering from the higher M portion of the distribution. In principle, a distribution of R_h in terms of mass fraction could be extracted from the distribution shown in Figure 8, assuming the same dependence of R_h on M as is observed for R_g, shown in Figure 5. However, the dependence of the measured intensity autocorrelation function on polydispersity is actually more complex, and a mass fraction distribution of R_h obtained in this manner would be quite unreliable.[28] We can observe

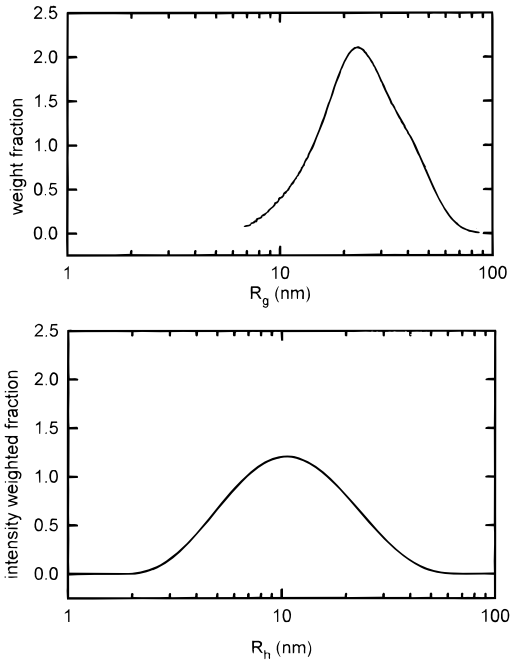

Figure 8. Distribution of R_g obtained by SEC/LS, and R_h obtained from dynamic light scattering for QZ1.

that both distributions shown in Figure 8 are monomodal and quite broad and that the maximum in the intensity-weighted distribution of R_h is very consistent with the second-order cumulant analysis above, R_h = 11 nm. This provides an estimate of the ratio R_g/R_h, of about 2. While this ratio is somewhat larger than is usually reported for flexible polymers, it is consistent with predictions for more extended polymers which are polydisperse and in good solvents.[29]

Equilibrium Molecular Structure. The repeat unit of QZ is completely 180° catenated, suggesting a rodlike conformation for the polymer. However, the dependence of R_g on M shown in Figure 5 shows an exponent near $^1/_2$, indicative of a random coil conformation, rather than an exponent near unity expected for rods. We have analyzed the SEC/LS data in terms of the Kratky−Porod wormlike chain model,[30] which encompasses the limits of rod (persistence length approaching infinity), and random coil (persistence length equal to one-half the Kuhn length). The plot in Figure 5 above shows the fit of the data to the Benoit−Doty expression for R_g of a wormlike chain:[31]

$$R_g^2 = \left(\frac{L l_k}{6}\right) - \left(\frac{l_k^2}{4}\right) - \left(\frac{l_k^3}{4L}\right)\left[1 - \left(\frac{l_k}{2L}\right)(1 - e^{-2L/l_k})\right] \quad (9)$$

where L is the maximum stretched-out length of the polymer molecule and l_k is the Kuhn statistical length. L is calculated from the molecular weight M using the so-called shift factor, or mass per unit length, M_L. Rather than use M_L as an adjustable parameter, we have estimated it as the mass of the repeat unit divided by the length of the repeat unit, using standard bond lengths. The curve shown in Figure 5 was obtained by setting M_L equal to 795 nm^{-1} and allowing l_k to vary to obtain the best fit. Values of l_k obtained in this manner varied from 27 to 32 nm for the samples measured. While this is an order of magnitude larger than is observed for polystyrene, it is far from the infinite value required for a "rigid rod" and is also much smaller than the stretched-out lengths of the polymer chains. At quite low M (<50 000) the polymers would begin to exhibit nearly rodlike conformations, but at the high M

investigated here, they can be described as coil-like. This is not immediately expected from the structure of the repeat unit, which is completely 180° catenated. Dilute solution measurements on a variety of apparently "rodlike" polymers, including poly(hexyl isocyanate),[25] poly(terephthalamide-*p*-benzohydrazide),[32] poly(*p*-benzamide),[33] poly(*p*-phenylenephthalamide),[34] and poly(*p*-phenylene-*cis*-benzobisoxazole),[35] have demonstrated that these polymers have persistence lengths of 30−60 nm. Molecular dynamics calculations done on a similar model backbone, poly(*p*-phenylene), also indicated less extended conformations than might intuitively be expected from the structure.[36] In the case of the poly(*n*-alkyl isocyanates), calculations showed that reasonable values of torsional and bond angle flexibility were sufficient to account for the observed equilibrium persistence length without the introduction of breaks.[37] These results suggest that a finite persistence length is an inherent property of even an apparently "rodlike" polymer. This limited persistence may also be reflected in the even smaller effective conjugation lengths[8,38,39] observed for conducting polymers. Although it has been suggested that this may be due to the existence of chemical defects and/or "twists" in the polymer chains,[41,42] the structural studies indicate that the limited electronic lengths may be at least partially due to inherent torsional flexibility. Energy migration studies on poly(*p*-phenyleneethynylene) polymers, including QZ, indicate a molecular weight of about 65 000 as a limiting M above which further enhancement in fluorescent quenching is not observed.[13] While this was only a relative measure of M, it is consistent with 2−3 Kuhn lengths. The evidence that the Kuhn statistical segment length is substantially smaller than the stretched-out length of the molecule suggests that the extended structure and high molecular weight of many of the conducting polymers may not be necessary to achieve the desired electronic properties. Introduction of flexible segments may improve processability without a loss in electronic properties. The copolymer approach, in which both the effective conjugation length and the structural flexibility can be controlled, has been investigated by several groups.[42−44]

Summary

The substituted poly(*p*-phenyleneethynylene) (QZ) has been synthesized at molecular weights which exceed 1 million. The data from classical intensity light scattering, size exclusion chromatography with a multiangle light scattering detector, and dynamic light scattering are all consistent with molecularly dispersed species of high M. The dependence of R_g on M over 2 decades is consistent with a wormlike chain model with a Kuhn statistical segment length of about 30 nm, when M_L is assumed to be 795 nm^{-1}. This length is substantially smaller than the stretched-out length of these high-M polymers, so that they exist as random coils in dilute solution. The statistical segment length of about 30 nm encompasses about 20 repeat units and is expected to be larger than the effective conjugation length for these polymers.

Acknowledgment. T.M.S. appreciates the financial support of the National Science Foundation MRL program (DMR-9120668), a NYI award (DMR-9258298), and a DuPont Young Professor Grant.

References and Notes

(1) Burroughes, J. H.; Bradley, D. D. C.; Brown, A. R.; Marks, R. H.; Friend, R. H.; Burn, P. L.; Holmes, A. B. *Nature* **1990**, *347*, 539.
(2) Czarnik, A. W., Ed. *Fluorescent Chemosensors for Ion and Molecular Recognition*; ACS Symposium Series 538; American Chemical Society: Washington, DC, 1993.
(3) Skotheim, T. J., Ed. *Handbook of Conducting Polymers*; Marcel Dekker: New York, 1986.
(4) Carter, F. L., Ed. *Molecular Electronic Devices*; Marcel Dekker: New York, 1982.
(5) Carter, F. L., Ed. *Molecular Electronic Devices II*; Marcel Dekker: New York, 1987.
(6) Kuzmany, H.; Mehring, M.; Roth, S., Eds. *Electronic Properties of Conjugated Polymers*; Springer: Berlin, 1987.
(7) Heeger, A. J.; Kivelson, S.; Schrieffer, J. R.; Su, W.-P. *Rev. Mod. Phys.* **1988**, *60*, 781.
(8) (a) Enkelman, V.; Wenz, G.; Muller, M. A.; Schmidt, M.; Wegner, G. *Mol. Cryst. Liq. Cryst.* **1984**, *105*, 11. (b) Wenz, G.; Muller, M. A.; Schmidt, M.; Wegner, G. *Macromolecules* **1984**, *17*, 837.
(9) Rawiso, M.; Aime, J. P.; Fave, J. L.; Schott, M.; Muller, M. A.; Schmidt, M.; Baumgarten, H.; Wegner, G. *J. Phys. Fr.* **1988**, *49*, 861.
(10) Xu, R.; Chu, B. *Macromolecules* **1989**, *22*, 3153.
(11) Garay, R.; Lenz, R. W. *Makromol. Chem. Suppl.* **1989**, *15*, 1.
(12) Zhou, Q.; Swager, T. M. *J. Am. Chem. Soc.* **1995**, *117*, 7017.
(13) Zhou, Q.; Swager, T. M. *J. Am. Chem. Soc.* **1995**, *117*, 12593.
(14) Kaye, W.; McDaniel, J. B. *Appl. Opt.* **1974**, *13*, 1934.
(15) Nagai, K. *Polym. J.* **1972**, *3*, 67.
(16) Berry, G. C. *Discuss. Faraday Soc.* **1970**, *49*, 121.
(17) Shukla, P.; Cotts, P. M.; Miller, R. D.; Russell, T. P.; Smith, B. A.; Wallraff, G. M.; Baier, M.; Thiyagarajan, P. *Macromolecules* **1991**, *24*, 5606.
(18) Zimm, B. H. *J. Chem. Phys.* **1948**, *16*, 1099.
(19) Debye, P. *J. Phys. Colloid Chem.* **1947**, *51*, 18.
(20) Mijnlieff, P. F.; Coumou, D. J. *J. Colloid Interface Sci.* **1968**, *27*, 553.
(21) Kato, T.; Miyaso, K.; Noda, I.; Fujimoto, T.; Nagasawa, M. *Macromolecules* **1970**, *3*, 777.
(22) Koppel, D. E. *J. Chem. Phys.* **1972**, *57*, 4814.
(23) Berne, B. J.; Pecora, R. *Dynamic Light Scattering*; John Wiley & Sons, Inc.: New York, 1976.
(24) Fujita, H. *Polymer Solutions*; Elsevier: New York, 1990.
(25) Murakami, H.; Norisuye, T.; Fujita, H. *Macromolecules* **1980**, *13*, 345.
(26) Jakes, J. *Czech. J. Phys.* **1988**, *B38*, 1305.
(27) Provencher, S. W. *Makromol. Chem.* **1979**, *180*, 201.
(28) Berry, G. C. In *Encyclopedia of Materials Science and Engineering*; Bever, M. B., Ed.; Pergamon Press: Oxford, 1986.
(29) Burchard, W. *Adv. Polym. Sci.* **1983**, *48*, 1.
(30) Kratky, O.; Porod, G. *Recl. Trav. Chim. Pay-Bas* **1949**, *68*, 1106.
(31) Benoit, H.; Doty, P. *J. Phys. Chem.* **1953**, *57*, 958.
(32) Sakurai, K.; Ochi, K.; Norisuye, T.; Fujita, H. *Polym. J.* **1984**, *7*, 559.
(33) Ying, Y.; Chu, B. *Macromolecules* **1984**, *20*, 871.
(34) Ying, Y.; Chu, B. *Makromol. Chem., Rapid Commun.* **1984**, *5*, 785.
(35) Roitman, D. B.; Wessling, R. A.; McAlister, J. *Macromolecules* **1993**, *26*, 5174.
(36) Socci, E. P.; Farmer, B. L.; Adams, W. W. *J. Polym. Sci., Polym. Phys. Ed.* **1993**, *31*, 1975.
(37) Cook, R. *Macromolecules* **1987**, *20*, 1961.
(38) Shand, H. L.; Chance, R. R.; Le Postollec, M.; Schott, M. *Phys. Rev. B* **1982**, *25*, 4431.
(39) Tain, B.; Zerbi, G.; Schenk, R.; Mullen, K. *J. Chem. Phys.* **1991**, *95*, 3191.
(40) Lim, K. C.; Fincher, L. A.; Heeger, A. J. *Phys. Rev. Lett.* **1983**, *50*, 1934.
(41) Halliday, D. A.; Burn, P. L.; Friend, R. H.; Bradley, D. D. C.; Holmes, A. B. *Synth. Met.* **1993**, *55−57*, 902.
(42) Burn, P. L.; Holmes, A. B.; Kraft, A.; Bradley, D. D. C.; Brown, A. R.; Friend, R. H.; Gymer, R. W. *Nature* **1992**, *356*, 47.
(43) Malliaras, G. G.; Herrema, J. K.; Wildeman, J.; Wieringa, R. H.; Gill, R. E.; Lampoura, S. S.; Hadziioannou, G. *Adv. Mater.* **1993**, *5*, 721.
(44) Yang, Z.; Sokolik, I.; Karasz, F. E. *Macromolecules* **1993**, *26*, 1188.

MA9602583